



# Isolation and characterization of novel micro cellulose from *Azadirachta indica* A. Juss agro-industrial residual waste oil cake for futuristic applications

Rantheesh J<sup>1</sup> · Indran S<sup>1</sup> · Raja S<sup>2</sup> · Suchart Siengchin<sup>3</sup>

Received: 12 August 2022 / Revised: 12 October 2022 / Accepted: 19 October 2022 / Published online: 7 November 2022  
© The Author(s), under exclusive licence to Springer-Verlag GmbH Germany, part of Springer Nature 2022

## Abstract

Every year, the food industry generates a large amount of waste, which prompts researchers to come up with a solution to efficiently manage the issue to support zero-waste concepts. After oil extraction, many oilseed cakes remain in the oil-processing industry as a waste. Converting this oilseed cake into value-added products would reduce environmental pollution and production costs. Oilseed cakes are high in fiber and contain a lot of non-starch polysaccharides. *Azadirachta indica* A. Juss neem oil cake (NOC) is a low-cost agricultural waste material produced during the oil extraction process of neem seeds. It is a dark brown powder that contains cellulose as well as other components such as hemicelluloses, proteins, and lipids. In this investigation, cellulose was extracted from the NOC, and comprehensive characterization was carried out. The polymer composite industry is in search of biofillers to incorporate with various matrices. As neem cake cellulose (NCC) is an entirely biodegradable material, it was considered for this study. To ensure its suitability in polymer composite industries, physicochemical, morphological, thermal, and spectroscopy analyses were carried out on NCC. Higher cellulose content (73.53%), better crystallinity (66.23%), lower density (1.59 g/cm<sup>3</sup>), considerable thermal stability (335.71 °C), kinetic activation energy (83.06 kJ/mol), particle size (17.93 μm), and good surface roughness (47.004 nm) make NCC suitable to be incorporated as a biofiller material in polymer matrices to manufacture eco-friendly composites.

**Keywords** Biomass · Biowaste · Biofiller · Neem oil cake · Cellulose

## 1 Introduction

In recent decades, cellulose has undoubtedly attracted the global market interest because it can be converted into micro- and nanomaterials with novel properties that are not found in bulk materials [1–3]. Cellulose is the most

abundant organic compound on the planet. It is basically derived from natural or synthetic sources. Natural cellulose is derived from plants, animals, and mineral sources. Synthetic cellulose is made from synthetic materials such as petrochemicals [4–7]. In its natural state, cellulose has a semi-crystalline structure with morphology and dimensions that vary depending on the origin and environment condition. As a biopolymer derived from natural resources, cellulose is getting much attraction for its renewable applications [8–12]. More advanced chemical, mechanical, as well as biological treatments are being developed for deriving cellulose from plant biomass [13–16]. Cellulose is being widely used in textile, pharmaceutical, chemical, paper, medical, and composite industries due to its biodegradability and biocompatibility [17, 18]. With a wider interest as a biomaterial, researchers have now proposed to use it as a material substitute for polymer matrix in various engineering areas [6, 19–21].

Cellulose is insoluble in water and most common solvents, owing primarily to the strong intramolecular and

✉ Indran S  
indransdesign@gmail.com

<sup>1</sup> Department of Mechanical Engineering, Rohini College of Engineering and Technology, Palkulam, Kanyakumari, Tamil Nadu 629 401, India

<sup>2</sup> Department of Mechanical Engineering, Noorul Islam Centre for Higher Education, Tamil Nadu, Kumaracoil 629180, India

<sup>3</sup> Natural Composites Research Group Lab, Department of Materials and Production Engineering, The Sirindhorn International Thai-German School of Engineering (TGGs), King Mongkut's University of Technology North Bangkok (KMUTNB), Bangkok, Thailand

intermolecular hydrogen bonding between individual chains. It is the main component of plant cell walls, contributing to the physical stability [6, 7, 11, 22, 23]. In plant cell walls, cellulose is linked with hemicellulose and lignin content covalent bonding and Van der Waals force. The quantities of the three components vary from 40 to 50%, 15 to 30%, and 20 to 30%. The crystalline structure of cellulose is a tightly packed chain with Van der Waals contacts and multiple intramolecular and intermolecular hydrogen bonding interactions. Degradability, hydrophilicity, chirality, and chemical inconsistency are all features of the cellulose molecule structure [12, 14, 16, 24, 25].

In the recent years, many studies have been carried out for development of bio-degradable micro- and nano-sized particles from a cellulose source for reinforcement in composites that would become a clear substitute for synthetic material derived composites used for structural applications [16, 18, 19, 26–28]. As a biofiller

to composites, cellulose offers attractive features such as good stiffness, better aspect ratio, low density, eco-friendly nature, and recyclability and ensures better mechanical properties than polymer composites [29, 30]. Apart from the above advantages, the production cost of biofillers is much lower than the synthetic counterparts [31, 32]. The major source for cellulose is wood, but its over exploitation is leading to deforestation and depletion of natural resources. According to literature, cellulose can be extracted from a variety of sources, including wheat straw, sugarcane straw, bagasse, hemp straws, flax straws, rice straw, rice husk, soybean hulls, jute, banana stems, pineapple leaf fiber, and palm oil residue as shown in Table 1. Research should also focus on finding alternate sources for cellulose extraction from biomass, agricultural residues, and industrial wastes.

Oilseed cakes are the major residues left over in oil industries and are classified as agroindustrial waste or

**Table 1** Physical and chemical properties of cellulose extracted from biomass

SI no	Cellulose S Cellulose source	Chemical properties					Physical properties		Reference
		Cellulose %	Hemi-cellulose %	Lignin %	Wax %	Ash %	Density g/cm <sup>3</sup>	Size µm	
1	NCC	96.53	2.58	0.87	-	0.02	1.59	12–14	Present study
2	Groundnut shells	82.7	6.05	0.34	-	-	-	-	[51]
3	Banana peel	74.24 ± 1.32	6.28 ± 0.08	10.18 ± 1.16	-	8.30 ± 1.23	-	19.2–30	[65]
4	Banana bract	78.53 ± 1.63	3.43 ± 0.21	1.59 ± 0.34	-	14.85 ± 1.15	-	15–45	[65]
5	Teff straw	89.9 ± 0.50	4.6 ± 0.20	3.1 ± 0.06	0.4 ± 0.01	0.6 ± 0.01	-	6.389 ± 2.24	[66]
6	Enset fiber	95.7 ± 0.41	2.3 ± 0.18	0.7 ± 0.01	0.2 ± 0.01	0.7 ± 0.28	-	13.37 ± 2.45	[66]
7	Sugarcane bagasse	90.8 ± 0.58	4.0 ± 0.38	2.8 ± 0.16	0.5 ± 0.01	0.7 ± 0.01	-	19.19 ± 5.18	[66]
8	Coffee hull	79.9 ± 0.46	8.8 ± 0.03	7.9 ± 0.14	0.9 ± 0.45	1.0 ± 0.01	-	24.06 ± 7.37	[66]
9	Peanut oil cake	82.3	9.4	7.6	-	0.5	1.58	15–25	[67]
10	Ficus leaf	90.6	2.5	4.7	-	1.1	-	-	[68]
11	African napier grass	93.5	2.9	3.4	-	-	-	8.3	[69]
12	Used disposal paper cups	90.2	4.2	1.8	3.7	-	-	15–20 13.7 ± 0.6 nm	[70]
13	Walnut shell	79.24 ± 2.51	0.28 ± 0.10	6.18 ± 1.24	-	14.30 ± 1.41	-	152.74 ± 5.87 µm	[71]
14	Corn cob	83.13 ± 2.63	1.59 ± 0.84	3.43 ± 1.17	-	11.85 ± 1.21	-	210.36 ± 7.49 µm	[71]
15	Sugarcane bagasse	85.57 ± 2.14	0.87 ± 0.21	4.76 ± 1.13	-	8.80 ± 1.06	-	218.65 ± 6.58 µm	[71]
16	Red banana tree, peduncles	89.5	8.2	2.3	-	-	-	-	[72]
17	Millet	85.2 ± 1.9	6.6 ± 1.2	4.9 ± 1.7	-	-	-	10–12 nm	[73]
18	Rice husk	73.8 ± 0.3	19.2 ± 0.7	1.6 ± 0.5	-	0.14 ± 0.03	-	-	[74]
19	Coffee husk	61.8 ± 2.6	27.2 ± 0.9	2.6 ± 0.4	-	0.49 ± 0.19	-	-	[74]
20	Areca nut husk fibre	85.47 ± 1.63	-	2.3 ± 1.04	-	-	-	1 nm	[75]
21	Mengkayang Leaves	81.6 ± 0.6	15.9 ± 0.6	0.8 ± 0.1	-	-	-	-	[40]
22	Helicteres isora plant	94.3 ± 3.3	0.6 ± 2.3	1.4 ± 3.2	-	-	-	-	[76]

by-products. The annual productivity of oilseed cake is estimated to be 0.145 million metric tonnes [33, 34]. Oilseed cakes can be classified as edible or nonedible. Edible oilseed cakes include mustard, sunflower, soybean, mahua, and peanuts. *Jatropha*, castor, neem, sesame, and simarouba, on the other hand, are considered nonedible oilseed cakes due to the presence of a high concentration of toxic compounds after the oil is extracted from the seeds.

Neem is a well-known source of nonedible oil. Oil can be extracted by passing or crushing the seed through a process used at 40–50 °C. Neem seed oil can also be obtained by solvent-extraction of the neem seed, fruit, oil cake, or kernel. Most industries extract the oil remaining in the seed using hexane. Neem cake is a by-product obtained in the solvent extraction method for neem oil. Being a totally botanical product, neem cake contains 100% natural NPK content along with various micronutrients. It is being used as an organic fertilizer, organic pesticide, organic insecticide, organic fungicide, etc. This is the first ever attempt made to derive cellulose from neem cake and to characterize the same for studying possibilities of using it as a biofiller for natural as well as synthetic composites. The cellulose was extracted from neem oil cakes (NOCs) using a low-cost chemical method. The extracted cellulose was investigated for its chemical structure by Fourier transform infrared (FTIR) spectroscopy. Crystallinity and thermal stability were found out using X-ray diffraction (XRD) and thermogravimetric analysis (TGA). The morphology was analyzed using scanning electron microscopy (SEM) and atomic force microscopy (AFM). Owing to its enhanced properties, the cellulose extracted from NOC can be used as a biofiller. It offers great mechanical strength and appreciable thermal resistance properties to the composite.

## 2 Materials and methodology

### 2.1 Materials

Neem cake was procured from a nonedible oil manufacturer located at Nagercoil, Kanyakumari district of Tamil Nadu, India. The direct purchase of neem cake from an oil mill guarantees that no preservatives were added. Chemicals such as hydrogen chloride (HCl), potassium chloride (KCl), hydrogen peroxide (H<sub>2</sub>O<sub>2</sub>), and sodium hydroxide (NaOH) were purchased from Sigma-Aldrich. All the chemicals used in the experiment were of analytical grade and were used exactly as received, with no further purification.

### 2.2 Extraction of cellulose from neem cake

#### 2.2.1 Pretreatment

Before pulverizing the NOC was dried in a hot-air oven at 50 °C until a constant weight was attained. With the help of a pulverizing machine, the NOC was ground to fine powder with particle size in micro ranges. Before the experimental analysis, the powder was stored in dark bags and kept in a dry and dark environment [35–37].

#### 2.2.2 Oil separation

Even after hot pressing or cold pressing with solvent extraction, the NOC will retain 10–20% of its oil content. This oil content removal is the first chemical procedure after pulverization. A pulp is created by combining oil cake powder and water in a proportionate amount. Then, 2 kg pulverized NOC powder is mixed up with 6 L water and is heated up to 80 °C for 2 h. The oil contents will be found suspended on the top layer of the solution, which is completely wiped off.

#### 2.2.3 Lignin separation

The remaining solution, which is almost free of soap content, is mixed with 4 L water along with half liter HCL and 100 g KCL. The new mixed solution is continuously heated up to 80 °C for 4 h. This helps to remove lignin and fatty-acid contents and to separate mineral contents. This will ultimately break the hemicellulose bond with cellulose. The solution obtained is continuously washed in distilled water until the pH becomes neutral.

#### 2.2.4 Hemicelluloses and phenolic content removal

The next procedure is to break up the chemical bondage between the cellulose, hemicellulose, and phenolic contents. For that 500 ml HCL along with 250 g KCL diluted in 250 ml water is mixed up for uniformity and is added with 6 L water. The solution is kept idle for soaking up to 12 h. After that, the content is then taken for hydrolysis further until the pH becomes neutral. The end solution has hemicelluloses, pectin along with cellulose separated as component items.

#### 2.2.5 Pretreatment/pre-bleaching

First, 200 ml hydrogen peroxide and 20 g Na(OH) is mixed with remaining content in 1 L water and the solution is

heated continuously up to 80 °C for 2 h. After observing foaming, the heating process is stopped, and then, hydrolysis is done until the solution becomes neutral. Thereafter, only cellulose content is remained.

### 2.2.6 Bleaching process

First, 2 sodium hypochloride is added to the remaining mixture and the solution is heated for 2 h at a temperature range of 60–80 °C. At the end, pure white cellulose is obtained as a residue. Thereafter, further hydrolysis is done to ensure purity. The obtained cellulose is dried under ambient conditions for moisture removal. The complete process of extracting cellulose from neem cake cellulose (NCC) is given Fig. 1.

## 2.3 Characterization techniques

### 2.3.1 Physical composition

The density and particle size of the extracted cellulose (NCC) were investigated to ascertain the critical physical parameters that determine its light-weight applicability. The density of the extracted NCC was measured by a pycnometer using toluene [4, 38]. The density was calculated using the following equation:

$$\rho_{NCC} = \frac{m_2 - m_1}{(m_3 - m_1)(m_4 - m_2)} \rho_t \quad (1)$$

where  $\rho_{NCC}$  is the NCC density (in kg/m<sup>3</sup>);  $m_1$  and  $m_2$  are pycnometer masses (in kg), before and after NCC filling;  $m_3$  is the pycnometer mass with toluene (in kg);  $m_4$  is the pycnometer mass filled with NCC and toluene (in kg); and  $\rho_t$  is the toluene density (866 kg/m<sup>3</sup>) at room temperature. The particle size of the NCC was determined with the help of SEM images and by analyzing the micrograph in the ImageJ software. A set of sample values were pointed and its mean value in micrometer was recorded. The yield of cellulose from the neem cake was calculated using the following equation:

$$\text{Percentage of cellulose yield in NCC} = \frac{W_2}{W_1} \times 100 \quad (2)$$

where  $W_1$  is the weight of neem cake sample before treatment and  $W_2$  is the weight of sample after the treatment.

### 2.3.2 Chemical composition

The chemical composition of the extracted cellulose was determined using the standard TAPPI (Technical Association of the Pulp and Paper Association) method [39, 40]. The lignin content was determined using the Kalson method and the TAPPI standard. The hollocellulose (cellulose + hemicellulose) content was determined according to TAPPI T 19 M-54. The  $\alpha$ -cellulose was removed from hollocellulose by alkali extraction. The hemicellulose fraction was calculated as the difference between the hollocellulose and  $\alpha$ -cellulose contents. The percentage

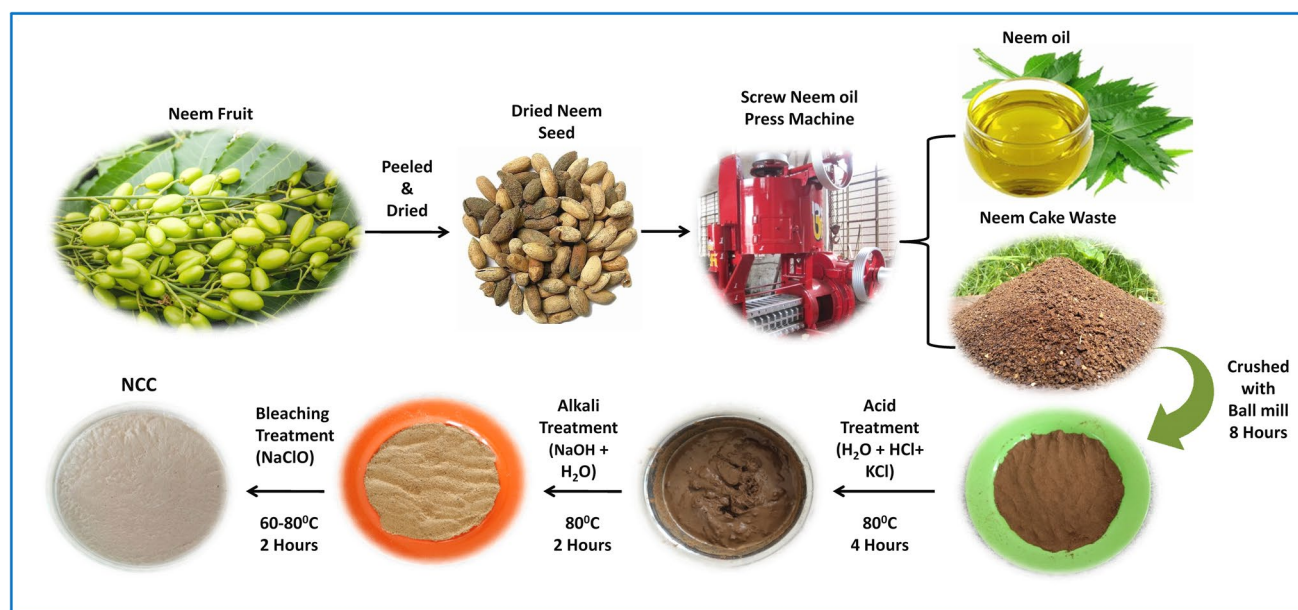


Fig. 1 Graphical representation of the process used to extract NCC

composition of  $\alpha$ -cellulose, hemicellulose, and lignin was determined and shown in Table 1. Moisture content was calculated by the statistical formula mentioned as Eq. (3) in which  $W_1$  represents the weight of undried cellulose sample containing moisture and  $W_2$  corresponds to the mass of moisture removed, dried cellulose.

$$\text{Moisture\%inNCC} = \left( \frac{W_1 - W_2}{W_1} \right) \times 100 \quad (3)$$

### 2.3.3 Thermogravimetric analysis

A thermogravimetric analyzer is used to measure the NCC's thermal performance. The TGA is carried out to predict the rate of change of weight with respect to temperature under the nitrogen environment. Cellulose extracted from NOC is subjected to thermal analysis using a thermogravimetric analyzer (model 6300; SIINT, Japan) under a chemically inert environment at a nitrogen flow rate of 20 ml per minute throughout analysis. Each set of samples was treated at 10 °C/min air. The change in masses was recorded for every 5 °C from 20 to 400 °C to ascertain the thermal stability of the neem cake–extracted cellulose. The changes in the mass of various chemical components of the fiber were documented in the form of TG/DTG curves and the thermal stability and maximum degradation temperature of the cellulose was labeled correspondingly. The kinetic activation energy ( $E_a$ ) of the NCC was calculated using Broido's equation to validate the NCC as reinforcement in a composite application [41–43].

$$\ln \left[ \ln \left[ \frac{1}{y} \right] \right] = - \left( \frac{E_a}{R} \right) \left[ \left( \frac{1}{T} \right) + K \right] \quad (4)$$

where  $y$  is the normalized weight ( $w_t/w_i$ ),  $w_i$  is the starting sample weight,  $w_t$  is the sample weight at time  $t$ ,  $R$  (8.32 J/mol K) is the gas constant,  $T$  is the temperature in Kelvin,  $K$  is the reaction rate constant, and  $E_a$  is the kinetic activation energy.

### 2.3.4 X-ray diffraction analysis

X-ray diffraction is a solid-state technique that can provide quantitative and qualitative information about the chemical structure of NCC. The crystalline parameters have a direct influence on the polymer material's tensile, thermal, and water absorption properties when they are used as fillers. The crystallographic structure of the cellulose samples (crystallinity index and crystallite size) was

recorded using DSXRD (Bruker). The diffraction spectra were magnified in the  $2\theta$  plane at a scan range of 10°–80° (room temperature) with a setting of 40 kv using CuK $\alpha$ . Ni-filtered radiation at an intensity of 1.5413 Å was used. The crystallinity index CI (%) and crystallite size (CS) were examined through Eqs. (5) and (6) with the help of Origin 2021 software.

$$\text{CI(\%)} = \frac{A_{\text{crystalline}}}{A_{\text{crystalline}} + A_{\text{amorphous}}} \times 100 \quad (5)$$

$$D = \frac{k\lambda}{\beta \cos\theta} \quad (6)$$

where  $A_{\text{amorphous}}$  is the area under amorphous curve region,  $A_{\text{crystalline}}$  is the area under crystalline curve region, and  $K$  refers to the Scherrer's constant (0.89). The representations  $\lambda$  and  $\beta'$  denote the wavelength of the X-ray and full-width at half-maximum of peak at 22.56°.  $D$  is the crystallite size (nm) and  $\theta$  is the diffraction angle (degree).

### 2.3.5 FTIR analysis

Chemical nature, existence of functional groups, and chemical bonds in the extracted cellulose were determined by FTIR spectroscopy [44, 45]. A spectrometer (FTIR-8400S; Bruker-Alpha, Germany) was used to perform the analysis. The NCC samples were irradiated with infrared light. It calculates the absorbance or transmittance against the wavenumber based on the absorption, transmission, and reflection of infrared light over the sample. The spectral analysis was performed in an absorbance range of 500–4000  $\text{cm}^{-1}$  at a resolution of 2  $\text{cm}^{-1}$  and scanning rate of 32 scans per minute. The FTIR spectra provide information on molecular vibrations, which aids in identifying the chemical and physical properties of the functional groups present in the sample.

### 2.3.6 SEM

SEM is a noncontact surface image capture technique used to measure NCC qualitatively (shape and structure) and quantitatively (size). The morphological and elemental composition analyses were carried out with the aid of a scanning electron microscope (SEM JEOL, USA) under 15 kV accelerating voltage. A thin layer of gold-coated samples was used for the purpose of preventing the accumulation of electric charges during the examination and thus ensuring the absolute conductivity of the materials. During the SEM image capture, an operating voltage of 10–15 kV was

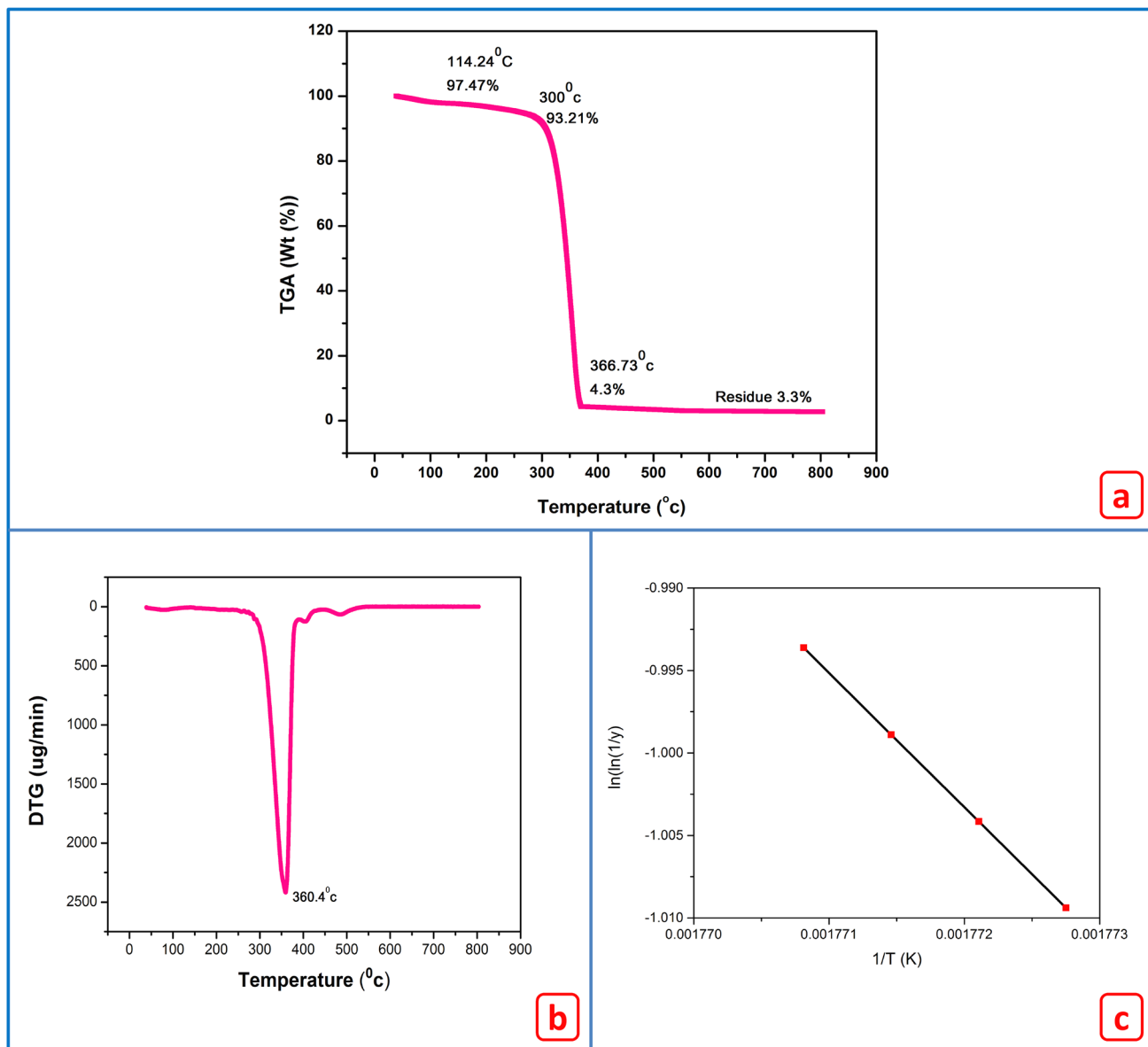


**Fig. 2** a TGA, b DTG, c Broidio's graph of NCC

maintained [46–50]. The ImageJ image-processing software was used for particle size analysis, and 19 particles were analyzed to extract the mean length (m) and shape descriptors.

### 2.3.7 EDX spectroscopy analysis

Energy-dispersive X-ray spectroscopy (EDX) is an approved element analysis technique for determining the chemical compositions of various elements such as

carbon, oxygen, nitrogen, sodium, and magnesium present on the surface of NCC and estimating their relative plentitude based on the intensity of the corresponding peaks [51, 52]. EDX was conducted on the cellulose samples for examining the presence of elements such as nitrogen, carbon, and oxygen. The test was performed on INCA Pental FETX3, which is equipped with an SEM machine. After analyzing the distribution of the elements present in the cellulose, their average values were considered.

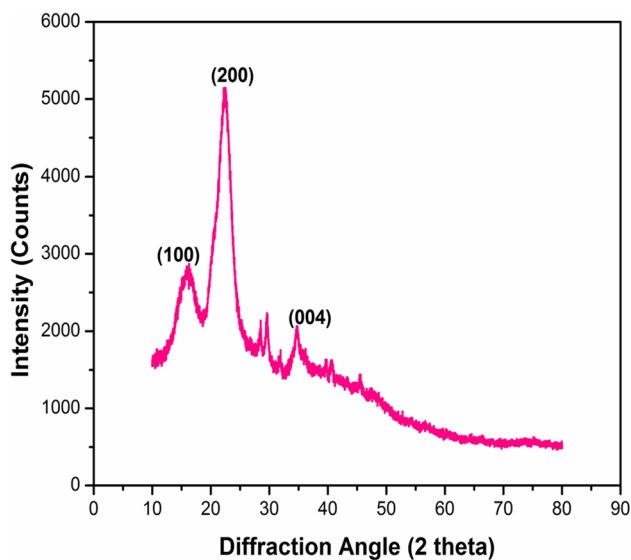


Fig. 3 XRD spectrum of extracted NCC

### 2.3.8 Atomic force microscopy

Atomic force microscopy was performed to ascertain the surface roughness ( $R_a$ ) of the cellulose samples with the help of XE70 C (Park System, Korea). AFM was equipped with a piezoelectric scanner with a tip radius of less than 10 nm. The equipment provided micrographs with a resolution of up to 1 nm. The obtained data were then analyzed to explain surface characteristics such as average roughness, roughness skewness ( $R_{sk}$ ), roughness kurtosis ( $R_{ku}$ ), 10-point roughness ( $R_z$ ), maximum peak-to-valley height ( $R_t$ ), and root mean square roughness ( $R_{rms}$ ).

## 3 Results and discussions

### 3.1 Physical composition analysis

The evaluation of NCC was necessary for recommending its usage as a biofiller with polymer matrix composites. Plants cellulose is a combination of  $\alpha$ - and  $\beta$ -cellulose and the density of 100% crystalline natural cellulose is between 1.582 and 1.599 g/cm<sup>3</sup> [53]. Using Eq. (1), it was found that the average density of the extracted NCC was 1.59 g/cm<sup>3</sup>, which correlated with the above findings. Alkali treatment eliminates lignin, hemicellulose, pectin, waxes, and contaminants [54, 55]. The amorphous portions were eliminated, leaving crystalline regions to enhance cellulose density [56]. Owing to their ordered and dense molecular structure, crystalline

areas may enhance stiffness, rigidity, and strength of the extracted NCC [57]. The bleaching treatment produced a cellulose-rich sample with a yield of  $68.73 \pm 1.13\%$  compared to the alkali treatment's yield of 88% from the neem cake sample. The yield content of various lignocellulosic wastes is as follows: kenaf stem (58 wt%), wheat straw (43 wt%), pineapple leaf (81 wt%), acacia bark (26 wt%), and banana rachis (48 wt%) [58–64].

### 3.2 Chemical composition analysis

Chemical composition and particle size of the extracted cellulose are listed in Table 1. The NCC have a considerable amount of cellulose content (up to 96.53%). Chemical composition analysis was performed to confirm richness of the cellulose content of NCC. Pretreatments, alkali treatment, and bleaching treatment yield a higher cellulose content. They promote the removal of noncellulosic components (i.e., as hemicellulose and lignin) in the NCC sample. The noncellulosic components are eliminated based on molecular weight and intermolecular bonding. In alkali treatment, hemicellulose–lignin connection breaks and partial delignification occur. An increase in NaOH concentration can break down cellulose molecules and change type I cellulose to type II cellulose. To avoid phase shift, mercerization is done with less alkali concentration (2%). The basic goal of pretreatment is to break the lignin structure in neem cake biomass and to make the residual polysaccharides more susceptible to additional treatments. The hydrophilic properties of neem cake and sodium hydroxide enhance the reaction rate and yield higher cellulose content. The alkali treatment increases interior surface area and decreases polymerization. It degrades lignin and carbohydrate bonds by saponifying intermolecular ester bonds. The lignin structure is broken by the glycosidic ether bond. The lignin degrades, making cellulose more fragile. Furthermore, bleaching removes the residual hemicelluloses, which cleaves the ester bond. On bleaching, lignin content further decreases. Delignification during bleaching is a vital step in cellulose extraction. Inside the cell wall, lignin acts as cement. By producing perhydroxyl anions that react with lignin's carbonyl groups, peroxide bleaching removes lignin. As a result, intermolecular bindings are minimized and lignin is eliminated. Less lignin and hemicellulose content in NCC enhance the potential for large-scale cellulose synthesis.

### 3.3 Thermogravimetric analysis

The TGA/DTG was used to evaluate the thermal degradation behavior of raw NCC. Figure 2a and b shows the resulting

**Table 2** The crystalline and thermal properties of various extracted cellulose

SI no	Cellulose source	Method of synthesis	Form of cellulose	Crystallinity index of cellulose (%)	Particle size	Yield	Thermal degradation			Reference
							Degradation of cellulose chain			
							50% degradation $T_{onset}$	Max degradation	Residue at 600 °C	
						%	°C	°C	%	
1	NCC	Chemical treatment	Cellulose	71	0.093–0.98 $\mu\text{m}$	68.73 $\pm$ 1.13	300	366.73	3.3	Present study
2	Rice husk	Chemical treatment	Cellulose	50	-	86	292.4 $\pm$ 0.6	326.8 $\pm$ 0.2	-	[74]
3	Dunchi fiber	Chemical treatment	Cellulose	66.70	-	23.2	225	330	-	[87]
4	Coffee husk	Chemical treatment	Cellulose	52	-	88	280 $\pm$ 3	315.6 $\pm$ 2	-	[74]
5	Tomato peels	Chemical treatment	Cellulose crystals	69	-	13.1	-	357	11%	[88]
6	Eggplant plant	Chemical treatment	Cellulose microfibrils	71	13.6 $\pm$ 2.5 $\mu\text{m}$	54	215	322	19	[84]
7	Millet husk	Chemical treatment and homogenization	Cellulose nanofibrils	58.5	-	65–70%	341	341	600 and 10.48	[73]
8	Corn husk	Chemical treatment	Cellulose microfibrils	53.7	733 $\pm$ 200 $\mu\text{m}$	-	-	-	-	[89]
9	Banana peel	Microwave digestion	Cellulose microfibrils	61.1	30 to 19.2 $\mu\text{m}$	55.48 $\pm$ 1.57%	201	214.65	368.11 and 8.96	[65]
10	Helicteres isora	Acid hydrolysis	Cellulose nanofibrils	88.68	-	40	-	-	-	
11	Areanut husk	Chemo-mechanical method	Cellulose nanofibrils	73	1 nm	22–26	262	369	500 and 15	[75]
12	Mengkuan leaves	Chemical treatment	Cellulose nanocrystals	69.5	5–80 $\mu\text{m}$	28	250	-	-	[40]
13	Rice straw	Chemical treatment	Cellulose microfibrils	68	-	12%	261	350	11%	[39]
14	Groundnut shells	Chemical treatment	Purified cellulose	68	-	43	253	330	2.54	[51]
15	Banana peel	Microwave digestion	Micro cellulose fiber	61.1	30 to 19.2 $\mu\text{m}$	55.48 $\pm$ 1.57	201	214.65	8.96	[65]
16	Banana bract	Microwave digestion	Micro cellulose fiber	28.6	-	64.67 $\pm$ 2.36	241.53	359.78	41.79	[65]
17	Hemp stalks	Chemical treatment	Cellulose microfibrils	76	16.96 $\mu\text{m}$	63	290	348	-	[90]
18	Red algae waste	Chemical treatment	Cellulose microfibrils	66	-	21.5	234	349	-	[91]
19	Vine shoots	Chemical treatment	Cellulose microfibrils	72	25 $\mu\text{m}$	-	287	326	-	[92]
20	Pineapple crown waste	Chemical treatment	Nano crystal	73	39 $\pm$ 12 nm	-	240	348	33.3%	[93]
21	Pea	Chemical treatment	Cellulose microfibrils	79	10.68 $\pm$ 1.28 nm	20	147	347	-	[94]
22	Broad beans	Chemical treatment	Cellulose microfibrils	70	14.67 $\pm$ 2.29 $\mu\text{m}$	18	247	333	-	[94]
23	Argan press cake	Chemical treatment	Cellulose	66.2	-	14	330.8	378.4	-	[95]
24	Teff straw (ts)	Chemical treatment	Celluloses	78	-	36.7	207.15	390.23	1.16	[66]
25	Enset fiber (ef),	Chemical treatment	Cellulose	85.56	-	60	210.43	400.22	18.07	[66]
26	Sugarcane bagasse (sb)	Chemical treatment	Cellulose	80.92	-	39.5	199.76	399.47	16.31	[66]
27	Coffee hull (ch)	Chemical treatment	Cellulose	77.59	-	35.5	282.45	390.20	16.61	[66]
28	Sunflower oil cake	Chemical treatment	Cellulose micro fiber	62	-	-	230	400	-	[96]
29	Alfa fibers	Chemical treatment	Cellulose micro fiber	71	-	-	235	354	-	[91]



**Table 2** (continued)

SI no	Cellulose source	Method of synthesis	Form of cellulose	Crystallinity index of cellulose (%)	Particle size	Yield	Thermal degradation			Reference
							Degradation of cellulose chain			
							50% degradation $T_{onset}$	Max degradation	Residue at 600 °C	
°C	°C	%								
30	Red banana tree, peduncles	Chemical treatment	Cellulose micro fiber	74.2	-	70	315	360	8%	[72]
31	figus leaf	Chemical treatment	Cellulose	55.9	-	55	290	370	4%	[68]
32	African napier grass	Chemical treatment	Cellulose	-	8.3	52	260	410	6.9	[69]
33	Date palm seeds	Chemical treatment	Cellulose	10.3	5 µm	97.3	230	400	10.3	[97]
34	Olive fiber	Chemical treatment	Microcrystalline cellulose	74.2	156.06 µm	-	286.1	359.1	23.6	[95]
35	Used disposal paper cups	Chemical treatment	Cellulose nanocrystals	86.5	13.7 ± 0.6 nm	76%	308	350	-	[70]
36	Walnut shell	Chemical treatment	Microcrystalline cellulose	65.22	152.74 ± 5.87 µm	35.36 ± 1.14%	260.96	362.42	19.85	[71]
37	Corn cob	Chemical treatment	Microcrystalline cellulose	49.58	210.36 ± 7.49 µm	27.24 ± 2.63	192.69	326.19	56.14	[71]
38	Sugarcane bagasse	Chemical treatment	Microcrystalline cellulose	70.64	218.65 ± 6.58 µm	32.12 ± 1.22	264.15	379.15	9.57	[71]
39	Bamboo	Hydrothermal	Cellulose	51.1	-	-	250	380	13.63	[98]
40	Cactus fruit waste seeds	Chemical treatment	Cellulose microfibrils	72	11	25	285.89	345.85	23	[55]
41	Steam exploded rice straw	Chemical treatment	Cellulose microfibrils	75.3	2–5 µm	-	261	350	-	[99]
42	Sugarcane Bagasse	Chemical treatment	Chemically purified cellulose	63.5	-	-	288	360	5.81	[100]

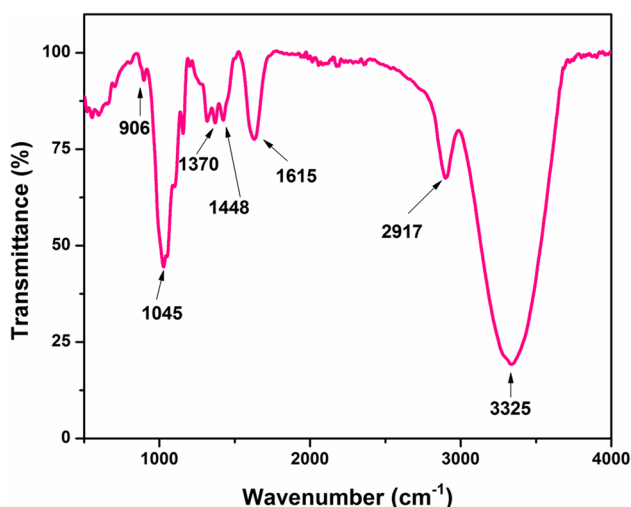


**Fig. 4** FT-IR spectrogram of extracted NCC

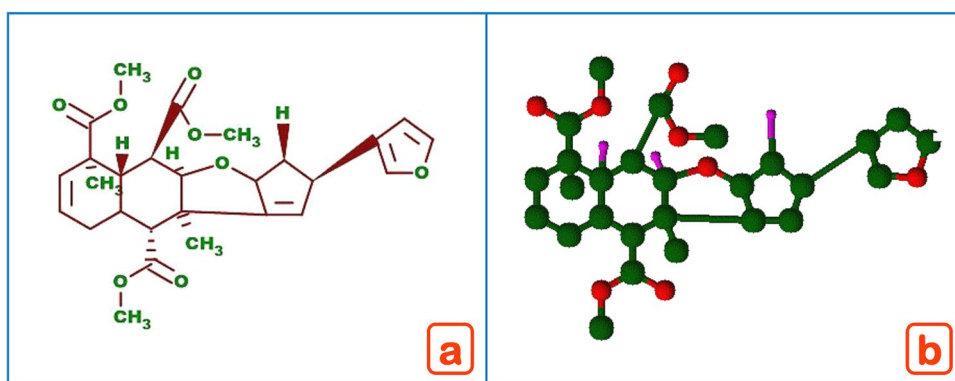
TGA and DTG curves. Because of the hydrophilic character of the cellulosic materials, NCC shows a slight weight loss at 100 °C due to evaporation of adsorbed moisture. In general, the thermal breakdown of lignocellulosic substance occurs in many steps due to the inclusion of various components with distinct degradation temperatures. The degradation of lignocellulosic material (hemicelluloses) begins at a lower temperature, followed by an early stage of lignin molecule destruction and subsequent cellulose decomposition. The extracted NCC components exhibit degradation peaks clustered in a single wide peak between 114.24 and 366.73 °C. Cellulose content in the NCC sample degraded in a single step between 300 and 366.73 °C, with a DTG maximum peak at 360.4 °C. This

breakdown is caused by cellulose degradation mechanisms such as dehydration, decarboxylation, depolymerization, and glycosyl unit disintegration. Moreover, the residue at 600 °C is found to 3.3%, which is very less, indicating complete elimination of noncellulosic components during bleaching [55, 77]. Thermal stability of NCC was determined by estimating kinetic activation energy ( $E_a$ ) using Eq. (4). Broidio's figure (Fig. 2c) was used to interpolate kinetic activation energy, and  $E_a$  was found to be 83.06 kJ/mol, which was within the range for natural cellulosic fillers (60–170 kJ/mol). Thus, the extracted NCC had a relatively good thermal stability and could withstand polymerization process effectively when used as filler for polymer composite [47, 78, 79].

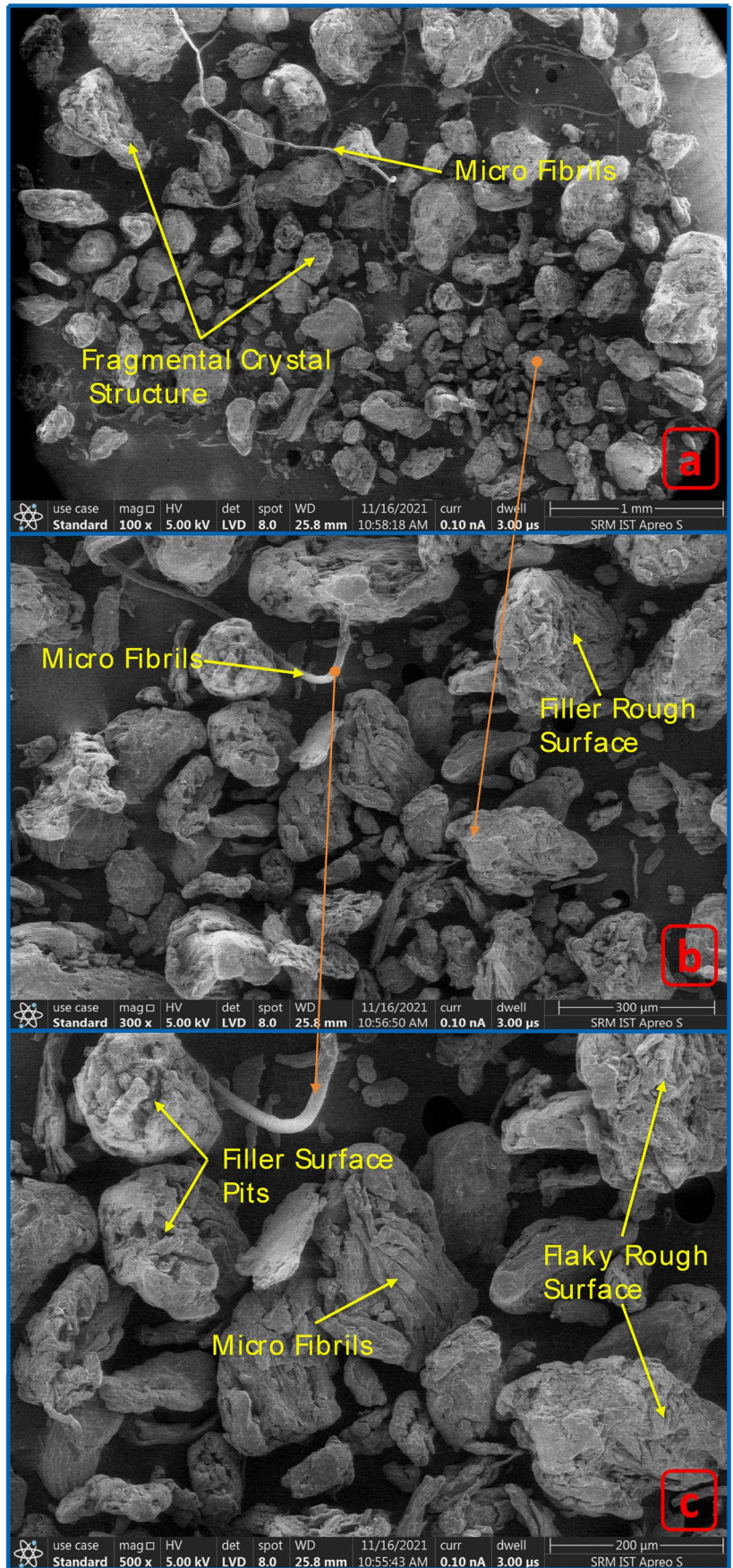
### 3.4 XRD analysis

Figure 3 shows the XRD spectra of the NCC. XRD analysis was carried out study the crystalline structure and crystallinity of cellulosic materials. The crystalline nature and the amount of crystallinity are shown by the sharpness and peak intensities [80]. All samples reveal the characteristic cellulose I structure, with crystalline peaks at 16.7°, 22.4°, and 34.6°, corresponding to (110), (200), and (004) reflection planes, respectively [81–83]. These peaks resemble the cellulose derivatives from lignocellulosic sources [84]. CI was calculated using the Segal Eq. (4). The CI of the NCC sample was 71%. The higher CI of the extracted cellulose compared to other derivative of celluloses (Table 2) confirms the effectiveness of hemicellulose depolymerization and delignification [85]. This happens because molecules of noncellulosic components (lignin and hemicelluloses) in the raw material are eliminated by chemical treatments (acid,

**Fig. 5** **a** 2D Chemical structure of extracted NCC; **b** 3D structure of NCC cellulose



**Fig. 6** a, b, and c SEM morphology images of NCC at different magnifications



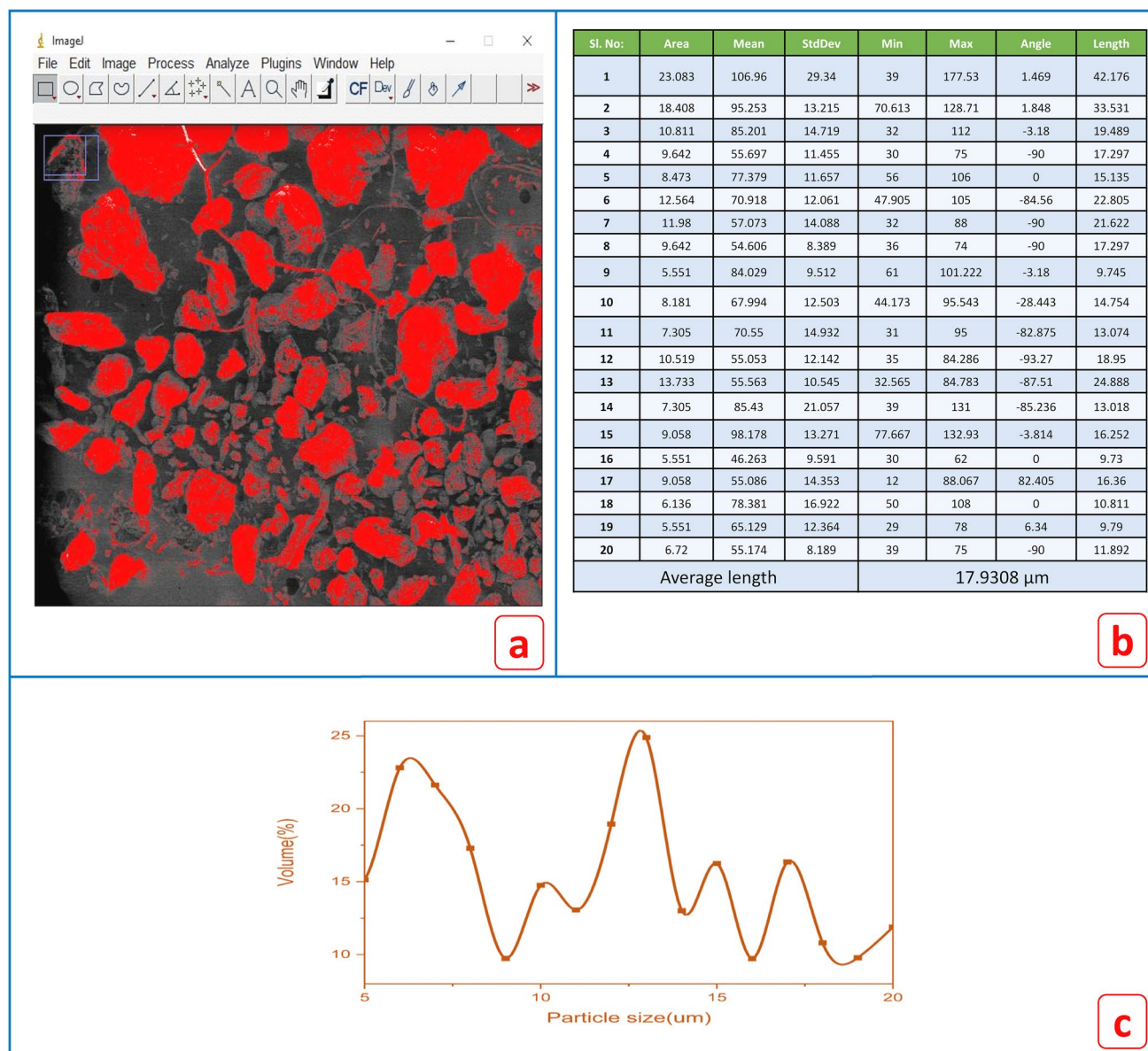


**Fig. 7** **a** ImageJ thresholding capture of the micro-cellulose particles, **b** particle size data, and **c** particle size distribution

alkali, and bleaching), which proved the effectiveness of treatment carried out in the cellulose extraction process. Using Eq. (5), we determined the crystallite size to be 42.03 nm. Higher CS enhances the hydrophobic character, which improves bonding capability if used as a filler for the polymer composite matrix [86].

### 3.5 FTIR analysis

FTIR spectroscopy is a common method used widely for knowing about the chemical structures of samples. The FTIR spectra of the chemically extracted NCC are shown

in Fig. 4. The sample displayed a large peak between 2900 and 3500  $\text{cm}^{-1}$  that indicates the free O–H stretching vibration of cellulose’s OH groups [75]. The sample’s spectra at around 2917  $\text{cm}^{-1}$  revealed the C–H stretching. The peak at 1370  $\text{cm}^{-1}$  was associated to the C–H and C–O bending. Pre-alkalization and alkalization remove hydroxyl groups by reducing hydrogen-bonding vibration. This is evident in O–H stretching vibration peak at 3325  $\text{cm}^{-1}$  [77]. Absorption peaks at 1615 and 1370  $\text{cm}^{-1}$  are due to cellulose’s C–C group [101]. The peak at 817  $\text{cm}^{-1}$ , whose functional group is C–Cl, indicates a minor impurity in the sample owing to bleaching treatment.

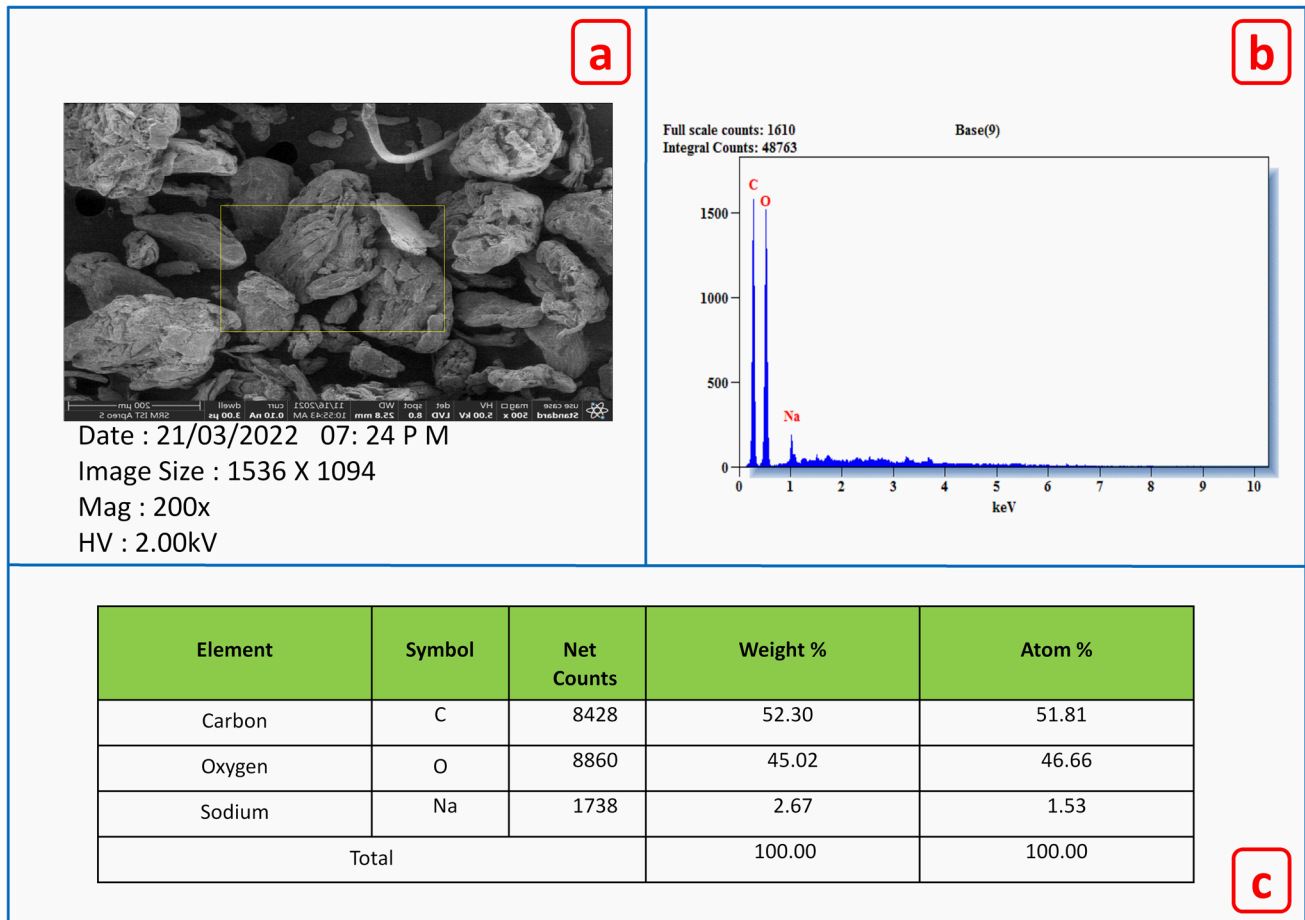


**Fig. 8** a EDX-SEM image and b EDX spectra and c elemental composition of NCC

The peak at  $1734.52\text{ cm}^{-1}$  is attributed to hemicelluloses, pectin, and waxes, whose intensity was lower, confirming the effective removal of these compounds after chemical treatment [40]. As lignin and hemicelluloses are present at a lower percentage, the peak at  $1045\text{ cm}^{-1}$  was caused by their ether linkage. The peak at  $906.86\text{ cm}^{-1}$  was attributed to  $\beta$ -glycosidic bonding of cellulose's glucose ring, perhaps due to acid treatment [73, 87]. Thus, the richness of the cellulose content in NCC proved the effectiveness of NaOH treatment and bleaching process in reducing the hemicellulose and lignin contents from the raw NOC. According to neem, there are an infinite number of possible chemical structures for extracted cellulose. Neem's medicinal properties can be found in every part of the plant. NCC chemical structure was outlined in Fig. 5a-2D and b-3D). The furanose formula explains this structure in detail. Each chain is linked by three  $\text{COOCH}_3$  molecules. For every single chain, there is

one chain with two  $\text{COOCH}_3$  molecules on each end. It was only at the cyclic structure's outer edge that the furan molecule was linked together. Neem had a distinct aroma, but it was not present all the time. In terms of chemical structure, it falls into the category of semi-aromatic. The presence of methyl groups in the ring adds complexity to the extracted NCC.

### 3.6 SEM morphology analysis

The SEM image of the chemically extracted cellulose is shown in Fig. 6. The micrographs clearly reveal the surface morphology of the cellulose. The samples were fragmented to micro-sized range due to the effect of chemical treatments [102].

The cellulose exists as small, fine crystals as a result of the penetration of hydronium ions into the amorphous

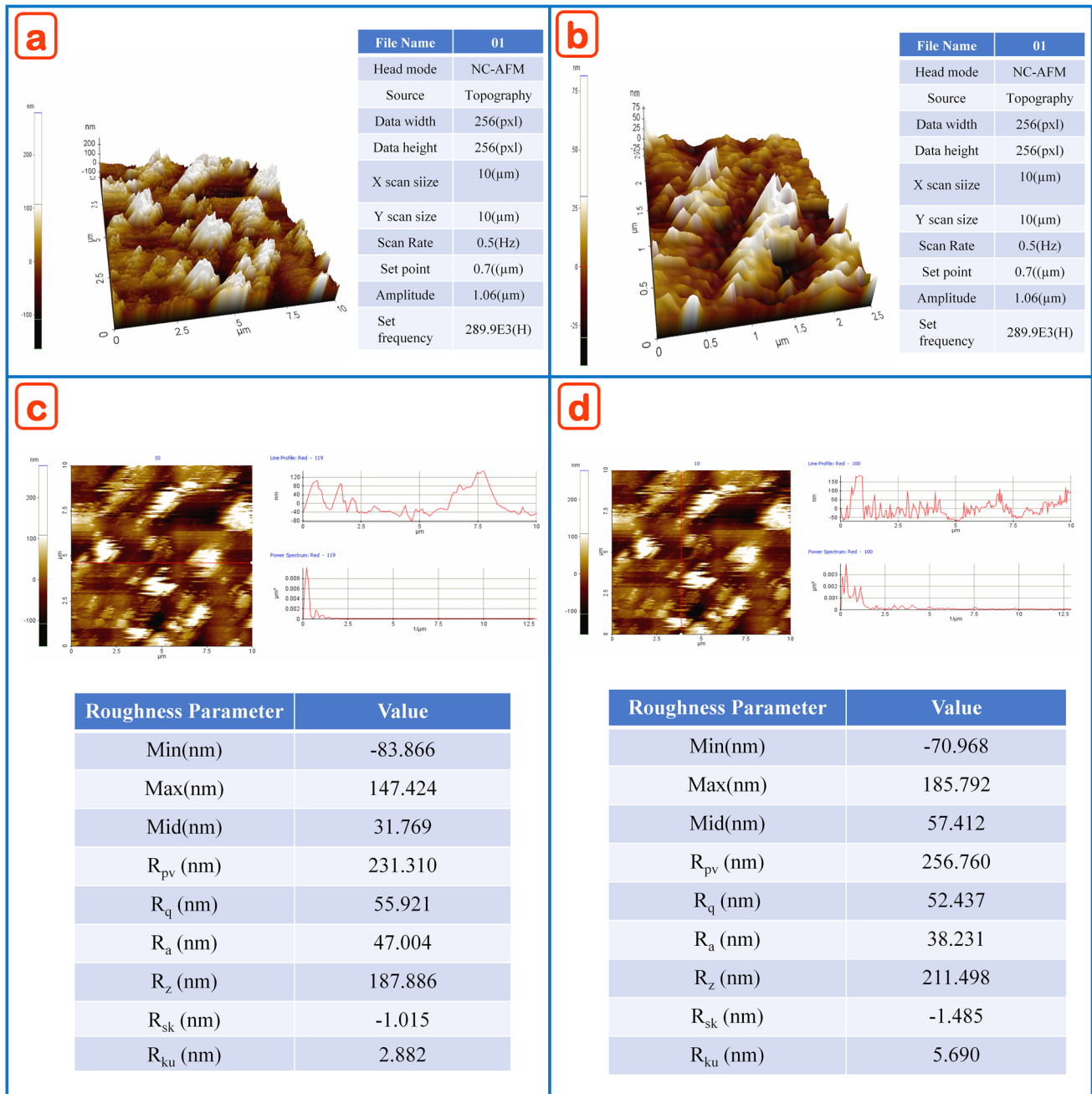


**Fig. 9** AFM outcomes of extracted NCC surface (**a&b** - 3D roughness view in horizontal and vertical probe move, **c&d** - 2D roughness view with observations in horizontal and vertical probe move)

regions of cellulose [103]. The noncellulosic components in NCC were dissolved by the bleaching as well as alkali and acid hydrolysis treatments. As a result, small pits and openings were seen, which increased the roughness of the extracted cellulose [73]. This roughness further makes

a good reinforcing material in fabrication of polymeric composites. The intersection method was used to find the mean particle size distribution [104]. The analysis of SEM image using the ImageJ software revealed that the particle size was in the 17.93 μm range, as shown in Fig. 7.

### 3.7 EDX analysis

NCC was analyzed for its elemental composition using EDX. From the spectra in Fig. 8, the presence of carbon, oxygen, and sodium corresponding to their binding energies can be identified. It is predominantly composed of 46.3 wt% oxygen, 52.4 wt% carbon, and 1.3 wt% sodium. The elemental impurity (Na) was due to the usage of NaOH acid in the chemical process. Although NCCs were washed several times, sodium was found in negligible amount. EDX examination revealed that NCC was very pure and without any other elemental impurities. In addition to carbon and oxygen, several researchers have found residues of potassium, salt, sulfur, and chlorine in the EDX spectra of cellulose extracted from other natural plant sources. This implies that the chemical treatments are highly effective for the removal of hemicellulose and lignin, resulting in the production of cellulose with a high degree of purity.

### 3.8 AFM analysis

AFM was used to ascertain the morphological topographies of NCC, which could be used for the determination of surface roughness. Figure 9 clearly demonstrates the 2D and 3D surface images of the NCC sample. The average roughness value ( $R_a$ ) of NCC is 47.004 nm. The negative skewness value ( $-1.015$ ) noted for NCC reveals the porous nature of the cellulose.

The surface kurtosis ( $R_{ku}$ ) value is 2.882, which is an indication of coarseness of NCC, which once again reveals NCC utilization as a biofiller [24, 30]. The other parameters were reported with values as average absolute height roughness ( $R_z = 187.856$  nm), root mean square surface roughness ( $R_q = 55.921$  nm), and the maximum peak valley height ( $R_t = 231.10$  nm). Better surface topographies are a clear indication for possibility of NCC being used as reinforcement in polymer composites in future.

## 4 Conclusion

In this study, a successful method was established for scientific extraction of cellulose from NOC. The chemical composition analysis of the extracted cellulose reported high cellulose percentage and minimal hemicelluloses, lignin, and moisture, which eventually make NCC a suitable biofiller for reinforcement recommendations. Evidence from FTIR, SEM, XRD, and TGA revealed that cementing components such as lignin, hemicellulose, and extractives had been removed. The XRD results confirmed that the newly extracted cellulose (NCC) possessed higher crystallinity. The SEM, EDX, and AFM analyses successfully

established the surface behavior of NCC, which was useful for developing good interfacial bonding when incorporated with polymer matrices. The thermal stability of the NCC was found promising in comparison to the existing cellulose reported so far. The degradation temperature of NCC was 337.71 °C, which is a clear hint for its future application as a biofiller even with thermoplastics whose processing temperature is up to 400 °C. Thus, this novel characterization study on industrial discarded NOC seems promising scope of sustainable development of a new biofiller (NCC) for the production of low-cost eco-friendly composites with economically better performance for a variety of structural and semi-structural applications.

**Acknowledgements** First author acknowledges the Rohini College of Engineering and Technology, Shiv Kumar—copyeditor, and Rado-ChemMAX, Nagercoil for providing research lab facilities to carry out his research work.

**Author contribution** Ranthesh J: conceptualization, investigation, methodology, writing—original draft, visualization, and data curation. S. Indran: resources, formal analysis, validation, writing—review and editing, project administration, and supervision. S. Raja: visualization and supported for data interpretation. Suchart Siengchin: resources and complete analysis of the work with technical correction.

**Data availability** The data that support the findings of this study are available on request from the corresponding author. The data are not publicly available due to privacy or ethical restrictions.

## Declarations

**Ethics approval** Not applicable.

**Competing interests** The authors declare no competing interests.

## References

1. Rangappa SM, Siengchin S, Parameswaranpillai J et al (2022) Lignocellulosic fiber reinforced composites: progress, performance, properties, applications, and future perspectives. *Polym Compos* 43:645–691. <https://doi.org/10.1002/PC.26413>
2. Miao C, Hamad WY (2013) Cellulose reinforced polymer composites and nanocomposites: a critical review. *Cellulose* 20:2221–2262. <https://doi.org/10.1007/s10570-013-0007-3>
3. Klemm D, Heublein B, Fink HP, Bohn A (2005) Cellulose: fascinating biopolymer and sustainable raw material. *Angew Chem Int Ed Eng* 44:3358–3393. <https://doi.org/10.1002/anie.200460587>
4. Somasundaram R, Rajamoni R, Suyambulingam I et al (2022) Utilization of discarded *Cymbopogon flexuosus* root waste as a novel lignocellulosic fiber for lightweight polymer composite application. *Polym Compos* 43:2838–2853. <https://doi.org/10.1002/PC.26580>
5. Divya D, Suyambulingam I, Sanjay MR, Siengchin S (2022) Suitability examination of novel cellulosic plant fiber from *Furcraea selloa* K. Koch peduncle for a potential polymeric composite reinforcement. *Polym Compos* 43:4223–4243. <https://doi.org/10.1002/PC.26683>

6. Thulasingh A, Kannaiyan S, Pichandi K (2021) Cellulose nanocrystals from orange and lychee biorefinery wastes and its implementation as tetracycline drug transporter. *Biomass Conv Bioref*. <https://doi.org/10.1007/s13399-020-01168-0>
7. Ran Y, Elsayed M, Eraky M et al (2022) Sequential production of biomethane and bioethanol through the whole biorefining of rice straw: analysis of structural properties and mass balance. *Biomass Convers Biorefin* 1:1–13. <https://doi.org/10.1007/S13399-022-02548-4>
8. Indran S, Raj RE, Daniel BSS, Saravanakumar SS (2016) Cellulose powder treatment on *Cissus quadrangularis* stem fiber-reinforcement in unsaturated polyester matrix composites. *J Reinforc Plast Compos* 35:212–227. <https://doi.org/10.1177/0731684415611756>
9. Sumesh KR, Kavimani V, Rajeshkumar G et al (2020) An investigation into the mechanical and wear characteristics of hybrid composites: influence of different types and content of biodegradable reinforcements. *J Nat Fibers* 00:1–13. <https://doi.org/10.1080/15440478.2020.1821297>
10. Alemdar A, Sain M (2008) Isolation and characterization of nanofibers from agricultural residues—wheat straw and soy hulls. *Biores Technol* 99:1664–1671. <https://doi.org/10.1016/j.biortech.2007.04.029>
11. Dube AM (2022) Isolation and characterization of cellulose nanocrystals from *Ensete ventricosum* pseudo-stem fiber using acid hydrolysis. *Biomass Convers Biorefin* 1:1–16. <https://doi.org/10.1007/S13399-022-02987-Z>
12. Barampouti EM, Christofi A, Malamis D, Mai S (2021) A sustainable approach to valorize potato peel waste towards biofuel production. *Biomass Convers Biorefin* 1:1–12. <https://doi.org/10.1007/S13399-021-01811-4/FIGURES/6>
13. Grishkewich N, Mohammed N, Tang J, Tam KC (2017) Recent advances in the application of cellulose nanocrystals. *Curr Opin Colloid Interface Sci* 29:32–45
14. Kumar A, Gupta V, Gaikwad KK (2021) Microfibrillated cellulose from pine cone: extraction, properties, and characterization. *Biomass Convers Biorefin* 1:1–8. <https://doi.org/10.1007/S13399-021-01794-2/FIGURES/6>
15. Zuluaga R, Putaux JL, Restrepo A et al (2007) Cellulose microfibrils from banana farming residues: isolation and characterization. *Cellulose* 14:585–592. <https://doi.org/10.1007/s10570-007-9118-z>
16. Arumugam M, Manikandan DB, Mohan S et al (2022) Comprehensive metabolite profiling and therapeutic potential of black gram (*Vigna mungo*) pods: conversion of biowaste to wealth approach. *Biomass Convers Biorefin* 1:1–32. <https://doi.org/10.1007/S13399-022-02806-5>
17. Wang Z, Yao ZJ, Zhou J, Zhang Y (2017) Reuse of waste cotton cloth for the extraction of cellulose nanocrystals. *Carbohydr Polym* 157:945–952. <https://doi.org/10.1016/j.carbpol.2016.10.044>
18. Eixenberger D, Carballo-Arce AF, Vega-Baudrit JR et al (2022) Tropical agroindustrial biowaste revalorization through integrative biorefineries—review part II: pineapple, sugarcane and banana by-products in Costa Rica. *Biomass Convers Biorefin* 1:1–28. <https://doi.org/10.1007/S13399-022-02721-9>
19. Mora-Villalobos JA, Aguilar F, Carballo-Arce AF et al (2021) Tropical agroindustrial biowaste revalorization through integrative biorefineries—review part I: coffee and palm oil by-products. *Biomass Convers Biorefin* 2021:1–19. <https://doi.org/10.1007/S13399-021-01442-9>
20. Cardoen D, Joshi P, Diels L et al (2015) Agriculture biomass in India: part I Estimation and characterization. *Resour Conserv Recycl* 102:39–48. <https://doi.org/10.1016/j.resconrec.2015.06.003>
21. Ubando AT, Felix CB, Chen WH (2020) Biorefineries in circular bioeconomy: a comprehensive review. *Bioresour Technol* 299:122585. <https://doi.org/10.1016/j.biortech.2019.122585>
22. Moshi AAM, Ravindran D, Bharathi SRS et al (2020) Characterization of a new cellulosic natural fiber extracted from the root of *Ficus religiosa* tree. *Int J Biol Macromol* 142:212–221. <https://doi.org/10.1016/j.ijbiomac.2019.09.094>
23. Arul Marcel Moshi A, Ravindran D, Sundara Bharathi SR et al (2020) Characterization of natural cellulosic fiber extracted from *Grewia damine* flowering plant's stem. *Int J Biol Macromol* 164:1246–1255. <https://doi.org/10.1016/j.ijbiomac.2020.07.225>
24. Arul Marcel Moshi A, Ravindran D, Sundara Bharathi SR et al (2020) Characterization of surface-modified natural cellulosic fiber extracted from the root of *Ficus religiosa* tree. *Int J Biol Macromol* 156:997–1006. <https://doi.org/10.1016/j.ijbiomac.2020.04.117>
25. Pardo RNC, Rojas GMA, Florez LM (2021) Thermal analysis of the physicochemical properties of organic waste to application in the compost process. *Biomass Conv Bioref*. <https://doi.org/10.1007/s13399-021-01786-2>
26. Huang G, Wu X, Hou Y, Cai J (2020) Sustainable porous carbons from garlic peel biowaste and KOH activation with an excellent CO<sub>2</sub> adsorption performance. *Biomass Convers Biorefin* 10:267–276. <https://doi.org/10.1007/S13399-019-00412-6/FIGURES/8>
27. Upadhyay A, Lama JP, Tawata S (2013) Utilization of pineapple waste: a review. *J Food Sci Technol Nepal* 6:10–18. <https://doi.org/10.3126/jfstn.v6i0.8255>
28. Stahel WR (2016) The circular economy. *Nature* 531:435–438. <https://doi.org/10.1038/531435a>
29. Karakoti A, Soundhar A, Rajesh M et al (2019) Enhancement of mechanical properties of an epoxy composite reinforced with *Hibiscus sabdariffa* var. *Altissima* fiber micro cellulose. *Int J Recent Technol Eng* 8:477–480. <https://doi.org/10.35940/ijrte.B1093.0782S419>
30. Soma Sundaram Pillai R, Rajamoni R, Suyambulingam I et al (2021) Synthesis and characterization of cost-effective industrial discarded natural ceramic particulates from *Cymbopogon flexuosus* plant shoot for potential polymer/metal matrix reinforcement. Springer, Berlin Heidelberg
31. Jabbar A, Militký J, Wiener J et al (2017) Nanocellulose coated woven jute/green epoxy composites: characterization of mechanical and dynamic mechanical behavior. *Compos Struct* 161:340–349. <https://doi.org/10.1016/j.compstruct.2016.11.062>
32. Sumesh K, Kavimani V, Rajeshkumar G, Indran S, Khan A (2022) Mechanical, water absorption and wear characteristics of novel polymeric composites: Impact of hybrid natural fibers and oil cake filler addition. *J Ind Textiles* 51(4\_suppl):5910S–5937S. <https://doi.org/10.1177/1528083720971344>
33. Mysiukiewicz O, Sałasińska K, Barczewski M, Szulc J (2020) The influence of oil content within lignocellulosic filler on thermal degradation kinetics and flammability of polylactide composites modified with linseed cake. *Polym Compos* 41:4503–4513. <https://doi.org/10.1002/PC.25727>
34. Elshaarani MT, Yaakob Z, Dahlan KZM, Mohammad M (2013) *Jatropha* deoiled cake filler-reinforced medium-density polyethylene biocomposites: effect of filler loading and coupling agent on the mechanical, dynamic mechanical and morphological properties. *Polym Compos* 34:746–756. <https://doi.org/10.1002/PC.22479>
35. Palanikumar V, Narayanan V, Vajjiram S (2018) Experimental investigation of mechanical and viscoelastic properties of *Acacia Nilotica* filler blended polymer composite. *Polym Compos* 39:2535–2546. <https://doi.org/10.1002/PC.24238>
36. Abu-Jdayil B, Mourad AH, Hassan M (2018) Development of polymeric heat insulators based on emirati red shale filler:



- thermal and physical properties. *Polym Compos* 39:E1463–E1473. <https://doi.org/10.1002/PC.24356>
37. Barman A, Shrivastava NK, Khatua BB, Ray BC (2015) Green composites based on high-density polyethylene and *Saccharum spontaneum*: effect of filler content on morphology, thermal, and mechanical properties. *Polym Compos* 36:2157–2166. <https://doi.org/10.1002/PC.23126>
  38. Indran S, Edwin Raj RD, Daniel BSS, Binoj JS (2018) Comprehensive characterization of natural *Cissus quadrangularis* stem fiber composites as an alternate for conventional FRP composites. *J Bionic Eng* 15:914–923. <https://doi.org/10.1007/s42235-018-0078-9>
  39. Razali NAM, Mohd Sohaiami R, Othman RNIR, Abdullah N, Demon SZN, Jasmani L, Yunus WMZW, Ya'acob WMHW, Salleh EM, Norizan MN, Halim NA (2022) Comparative study on extraction of cellulose fiber from rice straw waste from chemo-mechanical and pulping method. *Polymers* 14(3):387. <https://doi.org/10.3390/polym14030387>
  40. Sheltami RM, Abdullah I, Ahmad I et al (2012) Extraction of cellulose nanocrystals from mengkuang leaves (*Pandanus tectorius*). *Carbohydr Polym* 88:772–779. <https://doi.org/10.1016/j.carbpol.2012.01.062>
  41. Jenish I, Veeramalai Chinnasamy SG, Basavarajappa S et al (2020) Tribo-mechanical characterization of carbonized coconut shell micro particle reinforced with *Cissus quadrangularis* stem fiber/epoxy novel composite for structural application. *J Nat Fibers*. <https://doi.org/10.1080/15440478.2020.1838988>
  42. Rajeshkumar G, Hariharan V, Indran S et al (2020) Influence of sodium hydroxide (NaOH) treatment on mechanical properties and morphological behaviour of Phoenix sp. fiber/epoxy composites. *J Polym Environ* 29:765–774. <https://doi.org/10.1007/s10924-020-01921-6>
  43. Manimekalai G, Kavitha S, Divya D et al (2021) Characterization of enzyme treated cellulosic stem fiber from *Cissus quadrangularis* plant: an exploratory investigation. *Curr Res Green Sustain Chem* 4:100162. <https://doi.org/10.1016/j.crgsc.2021.100162>
  44. Jenish I, Veeramalai Chinnasamy SG, Basavarajappa S et al (2020) Tribo-mechanical characterization of carbonized coconut shell micro particle reinforced with *Cissus quadrangularis* stem fiber/epoxy novel composite for structural application. *J Nat Fibers* 00:1–17. <https://doi.org/10.1080/15440478.2020.1838988>
  45. Divya D, Jenish I, Raja S (2022) Comprehensive characterization of *Furcraea selloa* K. Koch peduncle fiber-reinforced polyester composites—effect of fiber length and weight ratio. *Adv Mater Sci Eng* 2022:1–10. <https://doi.org/10.1155/2022/8099500>
  46. Iyyadurai J, Gandhi VCS, Suyambulingam I, Rajeshkumar G (2021) Sustainable development of *Cissus quadrangularis* stem fiber/epoxy composite on abrasive wear rate. *Journal of Natural Fibers* 00:1–13. <https://doi.org/10.1080/15440478.2021.1982819>
  47. Gandhi VCS, Jenish I, Indran S, Rajan DY (2022) Mechanical and thermal analysis of *Cissus quadrangularis* stem fiber/epoxy composite with micro-red mud filler composite for structural application. *Trans Indian Inst Met* 75:737–747. <https://doi.org/10.1007/s12666-021-02478-1>
  48. Sari NH, Suteja, Ilyas RA, et al (2021) Characterization of the density and mechanical properties of corn husk fiber reinforced polyester composites after exposure to ultraviolet light. *Funct Compos Struct* 3. <https://doi.org/10.1088/2631-6331/ac0ed3>
  49. Sumesh KR, Kavimani V, Rajeshkumar G et al (2021) Effect of banana, pineapple and coir fly ash filled with hybrid fiber epoxy based composites for mechanical and morphological study. *J Mater Cycles Waste Manag* 23:1277–1288. <https://doi.org/10.1007/s10163-021-01196-6>
  50. Muthu chozharajan B, Indran S, Divya D et al (2020) Mechanical and thermal properties of *Chloris barbata* flower fiber / epoxy composites: effect of alkali treatment and fiber weight fraction. *J Nat Fibers* 00:1–14. <https://doi.org/10.1080/15440478.2020.1848703>
  51. Bano S, Negi YS (2017) Studies on cellulose nanocrystals isolated from groundnut shells. *Carbohydr Polym* 157:1041–1049. <https://doi.org/10.1016/j.carbpol.2016.10.069>
  52. Raja S, Rajesh R, Indran S et al (2021) Characterization of industrial discarded novel *Cymbopogon flexuosus* stem fiber: a potential replacement for synthetic fiber. *J Ind Text*. <https://doi.org/10.1177/15280837211007507>
  53. Penjumras P, Rahman RBA, Talib RA, Abdan K (2014) Extraction and characterization of cellulose from durian rind. *Agric Agric Sci Procedia* 2:237–243. <https://doi.org/10.1016/j.aaspro.2014.11.034>
  54. Babu BG, Princewinston D, Saravanakumar SS et al (2022) Investigation on the physicochemical and mechanical properties of novel alkali-treated *Phaseolus vulgaris* fibers. *J Nat Fibers* 19:770–781. <https://doi.org/10.1080/15440478.2020.1761930>
  55. Ait Benhamou A, Kassab Z, Boussetta A et al (2022) Beneficiation of cactus fruit waste seeds for the production of cellulose nanostructures: extraction and properties. *Int J Biol Macromol* 203:302–311. <https://doi.org/10.1016/j.ijbiomac.2022.01.163>
  56. Suksaeree J, Nawathong N, Anakkawee R, Pichayakorn W (2017) Formulation of polyherbal patches based on polyvinyl alcohol and hydroxypropylmethyl cellulose: characterization and in vitro evaluation. *AAPS PharmSciTech* 18:2427–2436. <https://doi.org/10.1208/s12249-017-0726-0>
  57. Heinze T, Camacho Gómez JA, Haucke G (1996) Synthesis and characterization of the novel cellulose derivative dansyl cellulose. *Polym Bull* 37:743–749. <https://doi.org/10.1007/BF00295772>
  58. Kocaman S, Karaman M, Gursoy M, Ahmetli G (2017) Chemical and plasma surface modification of lignocellulose coconut waste for the preparation of advanced biobased composite materials. *Carbohydr Polym* 159:48–57. <https://doi.org/10.1016/j.carbpol.2016.12.016>
  59. Kocaman S, Ahmetli G (2020) Effects of various methods of chemical modification of lignocellulose hazelnut shell waste on a newly synthesized bio - based epoxy composite. *J Polym Environ* 28:1190–1203. <https://doi.org/10.1007/s10924-020-01675-1>
  60. Fitriani F, Aprilia S, Arahman N et al (2021) Isolation and characterization of nanocrystalline cellulose isolated from pineapple crown leaf fiber agricultural wastes using acid hydrolysis. *Polymers (Basel)* 13(23):4188. Published 2021 Nov 30. <https://doi.org/10.3390/polym13234188>
  61. Li M, He B, Zhao L (2019) Isolation and characterization of microcrystalline cellulose from Cotton Stalk Waste. *Bioresources* 14:3231–3246. <https://doi.org/10.15376/biores.14.2.3231-3246>
  62. Abdul Rahman NH, Chieng BW, Ibrahim NA, Abdul Rahman N (2017) Extraction and characterization of cellulose nanocrystals from tea leaf waste fibers. *Polymers (Basel)* 9(11):588. Published 2017 Nov 7. <https://doi.org/10.3390/polym9110588>
  63. Perumal AB, Nambiar RB, Sellamuthu PS et al (2022) Extraction of cellulose nanocrystals from areca waste and its application in eco-friendly biocomposite film. *Chemosphere* 287:132084. <https://doi.org/10.1016/j.chemosphere.2021.132084>
  64. Ahuja D, Kaushik A, Singh M (2018) Simultaneous extraction of lignin and cellulose nanofibrils from waste jute bags using one pot pre-treatment. *Int J Biol Macromol* 107:1294–1301. <https://doi.org/10.1016/j.ijbiomac.2017.09.107>
  65. Harini K, Ramya K, Sukumar M (2018) Extraction of nano cellulose fibers from the banana peel and bract for production of acetyl and lauroyl cellulose. *Carbohydr Polym* 201:329–339. <https://doi.org/10.1016/j.carbpol.2018.08.081>
  66. Gabriel T, Belete A, Syrowatka F et al (2020) Extraction and characterization of celluloses from various plant byproducts. *Int*

- J Biol Macromol 158:1248–1258. <https://doi.org/10.1016/j.ijbmac.2020.04.264>
67. Sumesh KR, Kanthavel K, Kavimani V (2020) Peanut oil cake-derived cellulose fiber: Extraction, application of mechanical and thermal properties in pineapple/flux natural fiber composites. *Int J Biol Macromol* 150:775–785. <https://doi.org/10.1016/j.ijbmac.2020.02.118>
  68. Reddy KO, Uma Maheswari C, Muzenda E et al (2016) Extraction and characterization of cellulose from pretreated ficus (peepal tree) leaf fibers. *J Nat Fibers* 13:54–64. <https://doi.org/10.1080/15440478.2014.984055>
  69. Reddy KO, Maheswari CU, Dhlamini MS et al (2018) Extraction and characterization of cellulose single fibers from native african napier grass. *Carbohydr Polym* 188:85–91. <https://doi.org/10.1016/j.carbpol.2018.01.110>
  70. Nagarajan KJ, Balaji AN, Kasi Rajan ST, Ramanujam NR (2020) Preparation of bio-eco based cellulose nanomaterials from used disposal paper cups through citric acid hydrolysis. *Carbohydr Polym* 235:115997. <https://doi.org/10.1016/j.carbpol.2020.115997>
  71. Harini K, Chandra Mohan C (2020) Isolation and characterization of micro and nanocrystalline cellulose fibers from the walnut shell, corncob and sugarcane bagasse. *Int J Biol Macromol* 163:1375–1383. <https://doi.org/10.1016/j.ijbiomac.2020.07.239>
  72. Nagarajan KJ, Sanjay MR, Raghav GR, Anish Khan (2022) Extraction of cellulose nanocrystals from red banana peduncle agro-waste and application in environmentally friendly biocomposite film. *Polym Compos* 43(8):4942–4958.
  73. Midhun Dominic CD, Raj V, Neenu KV et al (2022) Chlorine-free extraction and structural characterization of cellulose nanofibers from waste husk of millet (*Pennisetum glaucum*). *Int J Biol Macromol* 206:92–104. <https://doi.org/10.1016/j.ijbiomac.2022.02.078>
  74. Collazo-Bigliardi S, Ortega-Toro R, Chiralt Boix A (2018) Isolation and characterisation of microcrystalline cellulose and cellulose nanocrystals from coffee husk and comparative study with rice husk. *Carbohydr Polym* 191:205–215. <https://doi.org/10.1016/j.carbpol.2018.03.022>
  75. Julie Chandra CS, George N, Narayanankutty SK (2016) Isolation and characterization of cellulose nanofibrils from arecanut husk fibre. *Carbohydr Polym* 142:158–166. <https://doi.org/10.1016/j.carbpol.2016.01.015>
  76. Joy J, Jose C, Varanasi SB et al (2016) Preparation and characterization of poly(butylene succinate) bionanocomposites reinforced with cellulose nanofiber extracted from *Helicteres isora* plant. *J Renew Mater* 4:351–364. <https://doi.org/10.7569/JRM.2016.634128>
  77. Reddy JP, Rhim JW (2018) Extraction and characterization of cellulose microfibrils from agricultural wastes of onion and garlic. *J Nat Fibers* 15:465–473. <https://doi.org/10.1080/15440478.2014.945227>
  78. Prabhu Stalin JRR, Jenish I, Indran S (2014) Tribological characterization of carbon epoxy composite materials with particulate silane treated SiC fillers. *Adv Mat Res* 984–985:331–335. <https://doi.org/10.4028/www.scientific.net/AMR.984-985.331>
  79. Sundaram RS, Rajamoni R, Suyambulingam I, Isaac R (2021) Comprehensive characterization of industrially discarded cymbopogon flexuosus stem fiber reinforced unsaturated polyester composites: effect of fiber length and weight fraction. *J Nat Fibers* 00:1–16. <https://doi.org/10.1080/15440478.2021.1944435>
  80. Zhao H, Kwak JH, Conrad Zhang Z et al (2007) Studying cellulose fiber structure by SEM, XRD, NMR and acid hydrolysis. *Carbohydr Polym* 68:235–241. <https://doi.org/10.1016/j.carbpol.2006.12.013>
  81. Senthil Muthu Kumar T, Rajini N, Obi Reddy K et al (2018) All-cellulose composite films with cellulose matrix and Napier grass cellulose fibril fillers. *Int J Biol Macromol* 112:1310–1315. <https://doi.org/10.1016/j.ijbiomac.2018.01.167>
  82. Kouadri I, Satha H (2018) Extraction and characterization of cellulose and cellulose nanofibers from *Citrullus colocynthis* seeds. *Ind Crops Prod* 124:787–796. <https://doi.org/10.1016/j.indcrop.2018.08.051>
  83. Nagarajan KJ, Ramanujam NR, Sanjay MR, Siengchin S, Surya Rajan B, Sathick Basha K, ..., Raghav GR (2021) A comprehensive review on cellulose nanocrystals and cellulose nanofibers: Pretreatment, preparation, and characterization. *Polym Compos* 42(4):1588–1630
  84. Bahloul A, Kassab Z, El Bouchti M, Hannache H, Oumam M, El Achaby M (2021) Micro- and nano-structures of cellulose from eggplant plant (*Solanum melongena* L.) agricultural residue. *Carbohydr Polym* 253:117311
  85. Agarwal UP, Ralph SA, Baez C et al (2017) Effect of sample moisture content on XRD-estimated cellulose crystallinity index and crystallite size. *Cellulose* 24:1971–1984. <https://doi.org/10.1007/s10570-017-1259-0>
  86. Kim SH, Lee CM, Kaffle K (2013) Characterization of crystalline cellulose in biomass: Basic principles, applications, and limitations of XRD, NMR, IR, Raman, and SFG. *Korean J Chem Eng* 30:2127–2141. <https://doi.org/10.1007/s11814-013-0162-0>
  87. Khan MN, Rehman N, Sharif A et al (2020) Environmentally benign extraction of cellulose from dunchi fiber for nanocellulose fabrication. *Int J Biol Macromol* 153:72–78. <https://doi.org/10.1016/j.ijbiomac.2020.02.333>
  88. Jiang F, Lo HY (2015) Cellulose nanocrystal isolation from tomato peels and assembled nanofibers. *Carbohydr Polym* 122:60–68. <https://doi.org/10.1016/j.carbpol.2014.12.064>
  89. Chen Q, Xiong J, Chen G, Tan T (2020) Preparation and characterization of highly transparent hydrophobic nanocellulose film using corn husks as main material. *Int J Biol Macromol* 158:781–789. <https://doi.org/10.1016/j.ijbiomac.2020.04.250>
  90. Kassab Z, Abdellaoui Y, Salim MH et al (2020) Micro- and nanocelluloses derived from hemp stalks and their effect as polymer reinforcing materials. *Carbohydr Polym* 245:116506. <https://doi.org/10.1016/j.carbpol.2020.116506>
  91. Kassab Z, Ben youcef H, Hannache H, El Achaby M (2019) Isolation of cellulose nanocrystals from various lignocellulosic materials: physico-chemical characterization and Application in Polymer Composites Development. *Mater Today Proc* 13:964–973. <https://doi.org/10.1016/j.matpr.2019.04.061>
  92. El Achaby M, El Miri N, Hannache H et al (2018) Production of cellulose nanocrystals from vine shoots and their use for the development of nanocomposite materials. *Int J Biol Macromol* 117:592–600. <https://doi.org/10.1016/j.ijbiomac.2018.05.201>
  93. Prado KS, Spinacé MAS (2019) Isolation and characterization of cellulose nanocrystals from pineapple crown waste and their potential uses. *Int J Biol Macromol* 122:410–416. <https://doi.org/10.1016/j.ijbiomac.2018.10.187>
  94. Kassab Z, Abdellaoui Y, Salim MH, El Achaby M (2020) Cellulosic materials from pea (*Pisum Sativum*) and broad beans (*Vicia Faba*) pods agro-industrial residues. *Mater Lett* 280:128539. <https://doi.org/10.1016/j.matlet.2020.128539>
  95. Hu Y, Hamed O, Salghi R et al (2017) Extraction and characterization of cellulose from agricultural waste Argan press cake. *Cellul Chem Technol* 51:263–272. <https://doi.org/10.1016/j.matpr.2021.07.030>
  96. Kassab Z, El Achaby M, Tamraoui Y et al (2019) Sunflower oil cake-derived cellulose nanocrystals: extraction, physico-chemical characteristics and potential application. *Int J Biol Macromol* 136:241–252. <https://doi.org/10.1016/j.ijbiomac.2019.06.049>
  97. Nabili A, Fattoum A, Passas R et al (2014) Extraction and characterization of cellulose from date palm seeds (*Phoenix dactylifera* L.). *Cellul Chem Technol* 50:9–10
  98. Lin Q, Huang Y, Yu W (2021) Effects of extraction methods on morphology, structure and properties of bamboo cellulose. *Ind Crops Prod* 169:113640. <https://doi.org/10.1016/j.indcrop.2021.113640>

99. Wang Z, Qiao X, Sun K (2018) Rice straw cellulose nanofibrils reinforced poly(vinyl alcohol) composite films. *Carbohydr Polym* 197:442–450. <https://doi.org/10.1016/j.carbpol.2018.06.025>
100. Kumar A, Singh Negi Y, Choudhary V, Kant Bhardwaj N (2020) Characterization of cellulose nanocrystals produced by acid-hydrolysis from sugarcane bagasse as agro-waste. *J Mater Phys Chem* 2:1–8. <https://doi.org/10.12691/jmpc-2-1-1>
101. Rehman N, Alam S, Amin NU et al (2018) Ecofriendly isolation of cellulose from eucalyptus lenceolata: a Rehman, N., Alam, S., Amin, N. U., Mian, I., & Ullah, H. (2018). Ecofriendly isolation of cellulose from eucalyptus lenceolata: A novel approach. *Int J Polym Sci* 2018. <https://doi.org/10.1155/2018/8381501>
102. Krishnamachari P, Hashaikeh R, Tiner M (2011) Modified cellulose morphologies and its composites; SEM and TEM analysis. *Micron* 42:751–761. <https://doi.org/10.1016/j.micron.2011.05.001>
103. Mtibe A, Linganiso LZ, Mathew AP et al (2015) A comparative study on properties of micro and nanopapers produced from cellulose and cellulose nanofibres. *Carbohydr Polym* 118:1–8. <https://doi.org/10.1016/j.carbpol.2014.10.007>
104. Trache D, Donnot A, Khimeche K et al (2014) Physico-chemical properties and thermal stability of microcrystalline cellulose isolated from Alfa fibres. *Carbohydr Polym* 104:223–230. <https://doi.org/10.1016/j.carbpol.2014.01.058>

**Publisher's note** Springer Nature remains neutral with regard to jurisdictional claims in published maps and institutional affiliations.

Springer Nature or its licensor (e.g. a society or other partner) holds exclusive rights to this article under a publishing agreement with the author(s) or other rightsholder(s); author self-archiving of the accepted manuscript version of this article is solely governed by the terms of such publishing agreement and applicable law.